CLEAN
Soil Air Water

Özge Hanay[1]
Ergin Taşkan[1]
Burçin Yıldız[1]
Halil Hasar[1]
Eoin Casey[2]

[1]Department of Environmental Engineering, Firat University, Elazığ, Turkey
[2]Department of Chemical and Bioprocess Eng., University College Dublin, Dublin, Ireland

Research Article

Gas/Substrate Fluxes and Microbial Community in Phenol Biodegradation Using an O_2-Based Membrane Biofilm Reactor

Phenol can be oxidized to the end products when oxygen is used as an electron acceptor. This study evaluated phenol oxidation in an oxygen-based membrane biofilm reactor (MBfR). The system achieved highest oxidation of both phenol and glucose when the phenol loading and glucose loading was ~4.7 and ~55 $g\,m^{-2}\,day^{-1}$, respectively. These conditions were sufficient to prove an O_2 flux of at least 46 $g\,O_2\,m^{-2}\,day^{-1}$. In the case of feeding solely with phenol, the MBfR accomplished the highest phenol oxidation (~100%) when the phenol loading was about $5.6 \pm 0.9\,g\,m^{-2}\,day^{-1}$ and the O_2 flux was higher than $13.4 \pm 2.2\,g\,O_2\,m^{-2}\,day^{-1}$. However, higher phenol loading could be compensated by a higher O_2 pressure, and the best performance occurred when the phenol loading was $5.6\,g\,m^{-2}\,day^{-1}$, the O_2 pressure was ~0.54 atm, and hydraulic retention time was 2.5 h. Membrane fouling caused a reduced O_2 flux, which led to low phenol-oxidation efficiency. However, the bacterial population present in MBfR was analyzed by PCR-denaturing gradient gel electrophoresis and a low biodiversity was found.

Keywords: Aerobic process; Gas flux; Membrane biofilm reactors; Microbial community; Phenol biodegradation

Received: September 12, 2012; *revised:* December 12, 2012; *accepted:* December 20, 2012

DOI: 10.1002/clen.201200414

1 Introduction

Phenol-containing streams are frequently discharged from many industries such as phenol-production, oil refineries, pesticide, fertilizer, explosive manufacturing, pharmaceutical, coal conversation, cooking plants, and dye manufacturing [1, 2]. In addition, phenolic compounds in water bodies can also be sourced from agricultural runoff and domestic activities [3]. They are, highly soluble and mobile in the liquid stream, can cause severe odor problems and are toxic to human and aquatic life. Due to its toxic effects on human health and the environment, the European Council Directive has set a limit of 0.5 μg/L to regulate phenol concentration in drinking water [4]. Up to now, many researchers have studied several methods such as physicochemical methods [5, 6], advanced oxidation processes [7, 8], biological processes [9, 10], and their combinations [11, 12] to remove phenols from environmental matrices. Physicochemical and advanced oxidation processes may be undesirable due to operating problems (e.g. the tendency for formation of secondary toxic materials such as chlorinated phenols) and high costs. Despite these problems, these methods have a role as a pre-treatment step to decrease the waste stream toxicity prior to biological aerobic or anaerobic treatment. Consequently, there has been an increasing interest in using biological processes for phenol treatment. The majority of these studies have been conducted using sequencing batch reactors (SBR) due to its flexibility of operation, compactness and easy control [9], and membrane bioreactors (MBR) due to complete biomass retention capacity and high biomass concentration [13, 14]. Microorganisms responsible for phenol degradation have a relatively low growth rate and consequently attached growth systems are favorable due to improved biomass retention [15]. The application of membrane biofilm reactors (MBfR) could improve performance of such attached growth systems for phenol biodegradation.

Oxygen-based MBfR is a novel technology whereby the biofilm is naturally immobilized on permeable membrane [16, 17]. Oxygen diffuses through the membrane into the biofilm where oxidation of pollutants, supplied at the biofilm–liquid interface takes place. The MBfR has several advantages such as, (i) bubbleless aeration which offers the potential for higher oxygen utilization efficiencies with consequent energy savings, (ii) simultaneous nitrification, denitrification, and chemical oxygen demand (COD) removal can be achieved [18, 19]. To our best knowledge, no previous work on the treatment of phenol using MBfR has been reported although a theoretical study has shown the potential of the MBfR in treating phenol compared to conventional biofilm processes [20]. In this study, a laboratory-scale MBfR was tested for phenol oxidation in solutions in the absence and presence of another organic source as glucose, considering the effect of some major factors such as phenol loading, oxygen pressure, and hydraulic retention time (HRT). In addition, the fluxes of glucose, phenol, and oxygen were evaluated according to the obtained results. PCR-denaturing gradient gel electrophoresis (DGGE) of 16S rRNA gene was used for monitoring the shift in bacterial community of aerobic MBfR during establishment of phenol biodegradation.

Correspondence: Dr. H. Hasar, Department of Environmental Engineering, Firat University, 23119-Elazığ, Turkey
E-mail: hhasar@firat.edu.tr

Abbreviations: **COD**, chemical oxygen demand; **DGGE**, denaturing gradient gel electrophoresis; **HRT**, hydraulic retention time; **MBfR**, membrane biofilm reactor; **MBR**, membrane bioreactor

2 Materials and methods

2.1 Experimental set-up

MBfR system comprised a membrane module of 32 hollow fiber gas-permeable membranes (Mitsubishi Rayon) placed inside a glass reactor with a liquid working volume of 0.250 L. Each hollow fiber membrane had an outer diameter of 280 μm. The fiber bundle has an active length of 17 cm to provide 47.85 cm^2 of membrane surface area in the reactor. Pure oxygen gas was supplied at set pressures of 0.27, 0.41, and 0.54 atm to the inside of the hollow fiber through the manifold at the base. The bulk liquid in the reactor was continuously mixed by the magnetic stirrer. The MBfR was covered with aluminum foil to avoid the growth of phototrophs. A peristaltic pump (Watson Marlow 205S) was used to feed the influent solution to the reactor. A schematic of the lab-scale MBfR used in this study is detailed by Hasar and Ipek [21].

Synthetic influent (per liter) consisted of: 0.08 g glucose, 165 mg $(NH_4)_2SO_4$, 0.25 mg $NaHCO_3$, 0.05 mg KH_2PO4, 0.05 mg $MgSO_4$ and 1 mL trace mineral solution. The trace mineral solution contained (per liter): 100 mg $ZnSO_4 \cdot 7\,H_2O$, 300 mg H_3BO_3, 200 mg $CoCI_2 \cdot 6\,H_2O$, 30 mg $MnCI_2 \cdot 4\,H_2O$, 30 mg Na_2SeO_3, 10 mg $CuCI_2 \cdot 2\,H_2O$ and 10 mg $NiCI_2 \cdot 6\,H_2O$.

2.2 Start-up and experimental conditions

The reactor was seeded with conventional activated sludge from the municipal wastewater treatment plant of Malatya, Turkey. Start-up of the reactor was initiated by seeding with 250 mL of inoculum. The inoculation liquid was mixed by the magnetic stirrer in the reactor for 72 h to establish the biofilm on the membrane surface under a pure oxygen pressure of 0.27 atm before the acclimation study began. The acclimation study was conducted by feeding glucose as the sole carbon source for five days and subsequently a mixture of glucose and phenol for a further 15 days. The initial phenol concentration was adjusted to 5 mg/L and first experiments were conducted at HRT of 10 h and oxygen pressure of 0.27 atm. Then the addition of glucose in the synthetic solution was discontinued and finally phenol, as the sole source of carbon was used the operation of reactor. The initial phenol concentrations were kept between 5 and 100 mg/L. The operating conditions are summarized in Tab. 1.

2.3 Analytical methods

All the liquid samples from the reactors were immediately analyzed. The analysis of phenol was performed at least two times by spectrophotometer (Jenway 6105). The absorbance of the colored complex of phenol and *p*-nitroaniline was read at 488 nm. Soluble COD was determined according to Standard Methods [22].

2.4 Molecular method

Total DNA was extracted from the MBfRs at different time intervals to reveal the changes in the microbial communities over time using DGGE analysis. DNA extractions were carried out with DNA isolation kit (PowerSoil) by considering manufacturer's instructions and then stored at −20°C. Fragments were amplified to nucleotide positions 341–534 of the *Escherichia coli* 16S rRNA gene sequence with the forward primer GC-BacV3f (5′-CGC CCG CCG CGC GCG GCG GGC GGG GCG GGG GCA CGG GGG GCC TAC GGG AGG CAG CAG-3′), and the reverse primer 534r (5′-ATT ACC GCG GCT GCT GG-3′). PCR amplification was performed using Thermocycler TECHNE/TC-512 with the program at previous study [23]. PCR products were controlled by 1% agarose gel electrophoresis prior to DGGE analysis. DGGE were run with 8% (w/v) polyacrylamide gel (acrylamide/bisacrylamide (37.5:1) stock solution, Bio-Rad) in TAE (40 mM Tris, 20 mM acetic acid, 1 mM EDTA, pH 8.3) with denaturing gradient ranging from 35 to 60% at 60°C with 100 V for 18 h. SYBR Gold solution was stained for 35 min and imagined by a Gel Monitoring System (Vilberlourmart). The excised DNA bands on DGGE gel were placed in sterile 1 mL vials, eluted into 20 mL of water and frozen at −20°C. Then, the sequence analysis for each product was performed after PCR was applied to the eluted DNA with the primers BacV3f without GC clamp and 534r using the same programs.

3 Theory and calculations

The removal capacity of each contaminant by biofilm can be obtained by flux analyses. The fluxes of each target contaminants were calculated using Eq. (1):

$$J = \frac{Q(S_0 - S)}{A_m} \tag{1}$$

where J is the flux (g m^{-2} day^{-1}) of target compound, Q is the influent flow rate (m^3/day), S_0, and S are the influent and effluent concentrations of the target compound (g/m^3), and A_m is the membrane or biofilm surface area (m^2).

The surface loading of the contaminant was calculated using the Eq. (2):

$$L_s = \frac{QS_0}{A_m} \tag{2}$$

Table 1. Experimental conditions at each periods

Variables	Period 1 (1–13 days)	Period 2 (14–22 days)	Period 3 (23–28 days)	Period 4 (29–42 days)	Period 5 (43–52 days)	Period 6 (53–61 days)	Period 7 (62–76 days)	Period 8 (77–87 days)	Period 9 (88–98 days)
Main carbon source	Glucose + phenol	Glucose + phenol	Glucose + phenol	Glucose + phenol	Glucose + phenol	Phenol	Phenol	Phenol	Phenol
COD from glucose (mg/L)	100	100	80	100	110	–	–	–	–
O_2 pressure (atm)	0.27	0.41	0.41	0.41	0.54	0.54	0.54	0.54	0.54
Influent phenol (mg/L)	5	5	10	10	10	10	50	100	100
HRT (h)	10	10	5	2.5	2.5	2.5	2.5	2.5	10

The oxidation of glucose occurs according to the following reaction neglecting biomass production when using glucose as the COD source:

$$C_6H_{12}O_6 + 6O_2 \rightarrow 6CO_2 + 6H_2O \quad (3)$$

The maximum oxygen demand from glucose oxidation can be estimated from the following equation:

$$J_{O_2\text{-}1} = 1.06 J_{glucose} \quad (4)$$

where $J_{O_2\text{-}1}$ is oxygen flux due to carbon demand (g $O_2\,m^{-2}\,day^{-1}$), $J_{glucose}$ is the organic removal flux (g COD $m^{-2}\,day^{-1}$); and 1.06 is stoichiometric coefficient, Y_O, (g O_2/g glucose). The Y_O value assumes that net biomass synthesis is small.

The oxidation of phenol occurs according to the following reaction neglecting biomass production when using phenol as the COD source:

$$2C_6H_6O + 14O_2 \rightarrow 12CO_2 + 6H_2O \quad (5)$$

In the case of complete phenol removal, system performance is easily determined by comparing the values of flux and surface loading because the surface load equals the flux of phenol. The oxygen flux for the oxidation of phenol can be calculated using Eq. (6):

$$J_{O_2\text{-}2} = 2.38 J_{phenol} \quad (6)$$

where $J_{O_2\text{-}2}$ is the oxygen flux required to oxidize phenol (g $O_2\,m^{-2}\,day^{-1}$) and J_{phenol} is the phenol flux as g $m^{-2}\,day^{-1}$. The value of 2.38 is the stoichiometric number of oxygen moles required for oxidizing each mol of phenol. Hence, the total flux of oxygen can be calculated using Eq. (7):

$$J_{O_2\text{-}T} = J_{O_2\text{-}1} + J_{O_2\text{-}2} \quad (7)$$

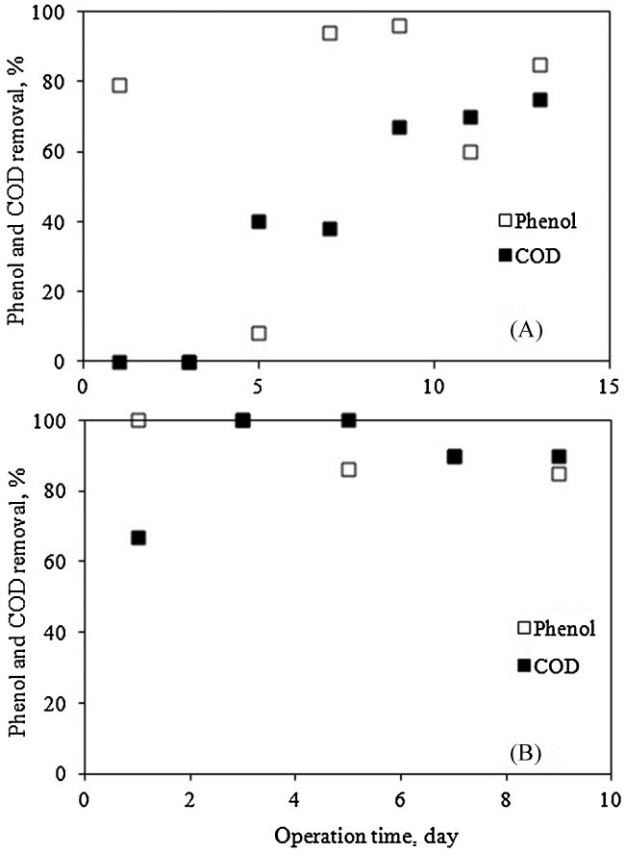

Figure 1. Phenol and COD removals; (A) Period 1: initial phenol concentration: 5 mg/L, P pressure: 0.27 atm and HRT: 10 h, (B) Period 2: initial phenol concentration: 5 mg/L, P: 0.41 atm, HRT: 10 h.

4 Results and discussion

4.1 Process performance

After biofilm in the MBfR was acclimated to both organic matter and phenol compound, the samples of influent and effluent were collected to determine process performance. Acclimation process took 20 days; an initial glucose feed for five days and a subsequent glucose and phenol mixture feed for 15 days. During period 1, the phenol removal began to increase after the 5th day of operation reaching 96% at the 9th day, as seen in Fig. 1. Separately COD removal reached 75% at the end of the 14-day experiment. Excellent results in both phenol and COD removals were obtained in period 2 in which initial phenol concentration, oxygen pressure and HRT was kept at 5 mg/L, 0.41 atm and 10 h, respectively. Phenol removals varied between 85 and 99.9% as COD was removed in the range of 67–90%. The results indicated that the phenol concentrations were <0.05 mg/L at 3rd and 5th days of operation, but increased to 0.75 mg/L within the later stages of period 2. Using a different reactor from MBfR, Dosta et al. [14] conducted a study on phenol removal using an aerobic MBR at low phenol concentrations in the range of 8 and 16 mg/L. They increased progressively the phenol loading by decreasing HRT and observed <1.0 mg phenol/L at the applied HRT in the range of 12 and 17 h. Barrios-Martinez et al. [24] reported 100% of phenol removal for petrochemical effluents by using an external MBR at low influent phenol concentration of 1.0 mg/L. This result demonstrated that low concentration of phenol did not have an inhibitory effect on the aerobic microorganisms.

Figure 2 indicates the phenol and COD removal at different HRTs and O_2 pressure levels between periods 3 and 5; periods have not been shown successively and each period has been started with first day on Figures. The influent phenol concentration was kept at 10 mg phenol/L during these periods. In the first of these periods (period 3), while the HRT was lowered from 10 to 5 h under the O_2 pressure of 0.41 atm, the phenol removal increased gradually up to 99.9%, however, the COD removal reached 70%. Both phenol and COD removals behaved in an opposing trend when only the HRT was dropped to 2.5 h in period 4, for example, the phenol removal increased while the COD removal decreased until the 11th day of operation. Yet, both COD and phenol removals deteriorated at advancing days. Therefore, the O_2 pressure was raised to 0.54 atm in period 5, while maintaining all the parameters of the previous period. Unfortunately, phenol and COD removal did not exhibit a stable behavior; the COD removal decreased while phenol removal increased. The phenol removal was approximately 25% as the COD removal reached 99.9% at the end of period 5. It was unlikely that the imposed phenol concentration resulted in inhibition of biological activity since the phenol removal efficiency reached 99.9% in terms of phenol. Over time, it was observed that the biofilm thickness increased rapidly. This is a potentially problematic situation for biofilm activity in the MBfR.

CLEAN Soil Air Water

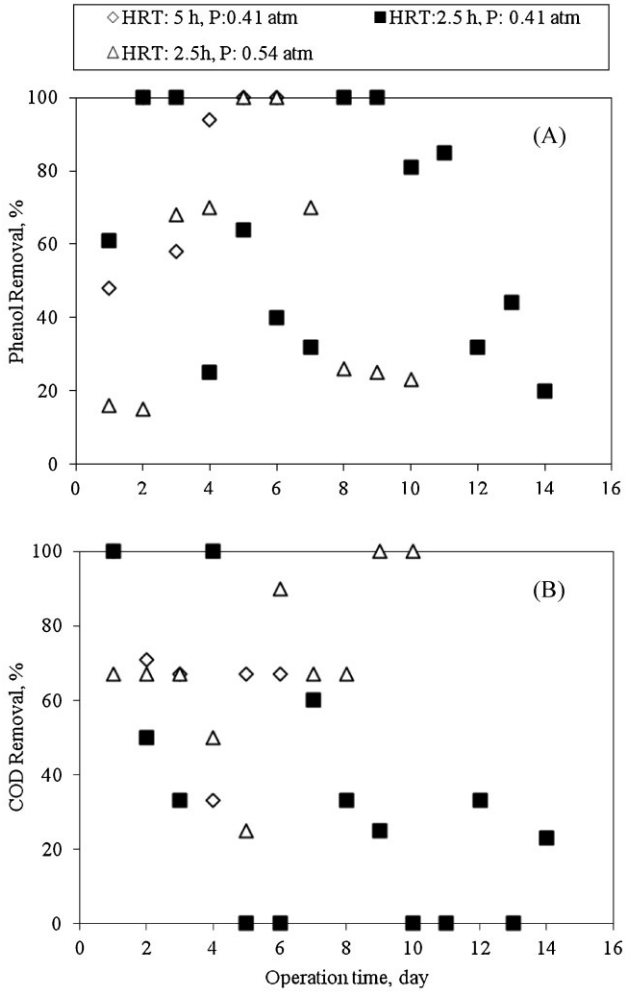

Figure 2. Phenol and COD removal. Initial phenol concentration: 10 mg/L, feeding with glucose. Period 3 (◇); P:0.41 atm, HRT:5 h, Period 4 (■); P:0.41 atm, HRT:2.5 h, Period 5 (Δ); P: 0.54 atm, HRT:2.5 h.

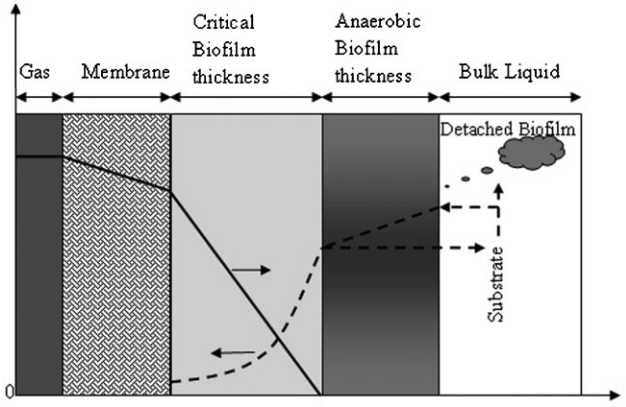

Figure 3. The role of biofilm thickness in MBfR.

With increasing biofilm thickness, aerobic conditions will be maintained near the membrane surface and anaerobic conditions that in the present study were indicated by a brown-black biofilm, will prevail near the biofilm liquid interface. Moreover, biofilm thickness control is the most significant challenge for the oxygen based MBfR because excessive biofilm causes flow misdistribution in the membrane module with consequent channeling and clogging. As shown schematically in Fig. 3, oxygen and soluble substrate are supplied from opposite sides of the biofilm. The aerobic region occurs where oxygen and substrates and/or nutrients are simultaneously available within the biofilm. It is speculated that a significant fraction of the biofilm, corresponding to the anaerobic layer, detached and was released to the bulk liquid. This may have accounted for the performance deterioration as shown in Fig. 2. In the MBfR, the location of maximum microbial activity may occur anywhere within the depth of membrane supported biofilm and is dependent on the relative supply level of oxygen and organic substrate supplied form the opposing sides of the biofilm [25]. The excessive biofilm, appeared brown-black, was removed by washing with liquid followed skimming with fingers by using sterile gloves. This solution unfortunately causes a decrease in the system performance. Recently, Hwang et al. [19] reported that optimum biofilm thickness would vary with substrate type, concentration, gas type, gas pressure, fiber spacing, and gas delivery mechanism. The MBfR technology uses a completely different oxygen delivery mechanism compared to conventional biofilm reactors. A few studies demonstrated that the biofilm thickness in the MBfR varied according to substrate and bacteria type. For example, Satoh et al. [26] reported that the biofilm thickness achieved up to 2100 μm for COD removal and nitrification while Hwang et al. [19] reported that the biofilm thickness solely reached 270 μm for denitrification with H_2. In a study by Downing and Nerenberg [27], biofilm thickness was controlled at 120 μm using nitrogen sparging to limit oxygen transfer for COD removal and nitrification. It is clear that in MBfRs, the biofilm thickness is a critical and potentially limiting parameter.

Phenol being a source of carbon for bacteria, the biofilm was acclimated by increasing the initial phenol concentration from 10 to 50 mg/L over time. In periods 6 and 7, phenol as a sole carbon source was used in the MBfR operated under the conditions of 2.5 h of HRT and 0.54 atm of O_2 pressure. Increasing the initial concentration of phenol unfortunately caused a decrease in the phenol removal, as seen in Fig. 4. While phenol removal reached almost 99.9% at an initial phenol concentration of 10 mg/L, it varied between 26 and 84% at initial phenol concentration of 50 mg/L. On the other hand, it was observed that COD removal exhibited a similar behavior with phenol removal profile. When the initial phenol concentration (period 8) was increased to 100 mg/L under O_2 pressure of 0.54 atm, the results showed that both the removals of COD and phenol were lower than previous conditions (Fig. 5). At a HRT of 2.5 h, the removals were observed to be in the range of 10 and 30% for phenol and 10 and 37% for COD. It was shown that increasing the HRT (period 9) did not provide a significant contribution for improving to the removal of phenol and COD. Unfortunately, phenol concentrations higher than 50 mg/L decrease considerably the efficiency of MBfR in phenol removal.

To further understanding of phenol biodegradation process, the microbial composition of acclimatized consortium in periods 3 (band B) and 6 (band A) was analyzed by PCR-DGGE. Although only few clones of each samples were sequenced, it was shown that the use of molecular biology techniques based on 16 sRNA gene sequences could identify microorganisms in hetetrophic biofilm. The results indicated that the consortium had same microbial composition and low diversity during phenol biodegradation, as seen in Fig. 6. Three species extracted from DGGE bands were sequenced

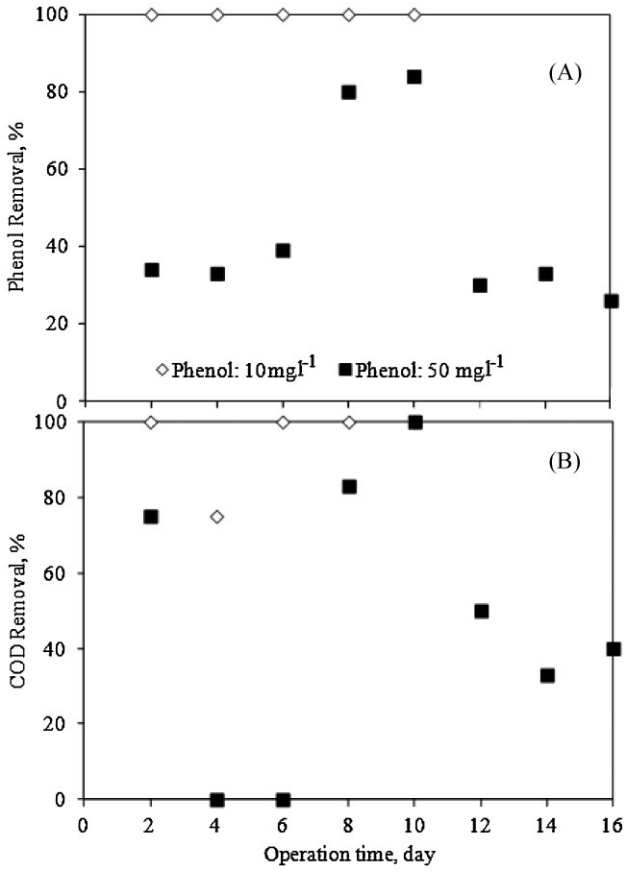

Figure 4. Phenol and COD removal. HRT: 2.5 h, P: 0.54 atm, only feeding with phenol. Period 6 (◇); phenol: 10 mg/L, period 7 (■); phenol: 50 mg/L.

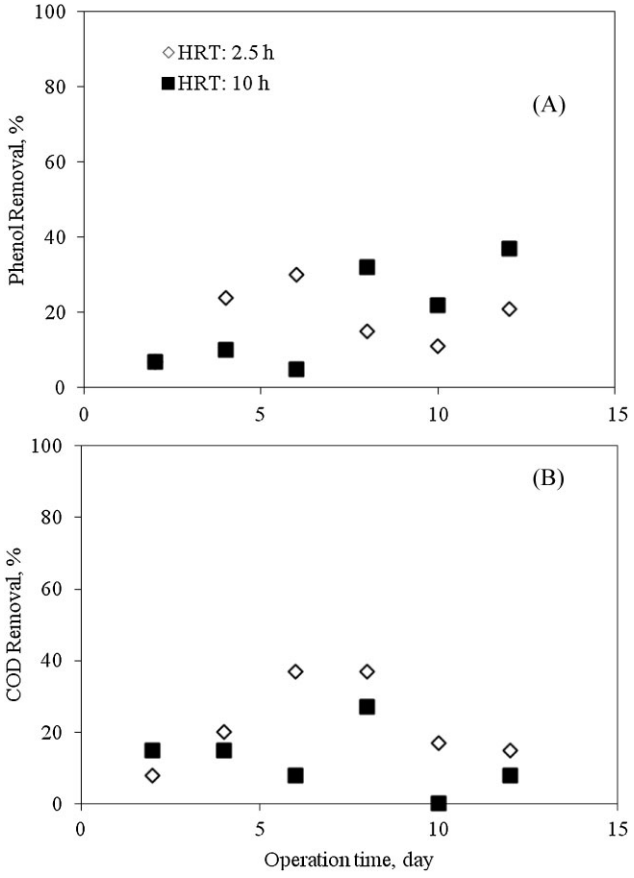

Figure 5. Phenol and COD removal. P: 0.54 atm, initial phenol concentration: 100 mg/L. Period 8 (◇); HRT:2.5 h, period 9 (■); HRT: 10 h.

and compared with the published species in NCBI. Based on the 16S rDNA gene library results, the consortium was prodominated by Gammaproteobacteria (67% of colones, bands 1 and 3) and Betaproteobacteria (33% of colones, band 2). The BLAST analysis of colones sequences from bands showed the representation of clones with 95% identity to *Dechloromonas* sp. (reference no: AY126452), 100% identity to *Klebsiella* sp. (ref. no: JN987862) and 100% identity to *Pseudomonas* sp. (ref no: HM192790). Nerenberg et al. [28], isolated *Dechloromonas* sp. from a hydrogen-based autotrophic hollow fiber MBfR that was actively reducing 5 mgN/L nitrate and around 1 mg/L perchlorate [28]. Nerenberg et al. [28] reported that *Dechloromonas* sp. can grow autotrophically with hydrogen as an electron donor and heterotrophically with acetate. In current study, it was shown that it can also grow heterotrophically with glucose + phenol or only phenol as electron donor because MBfR was operated with glucose + phenol at period 3 and only phenol at period 6. On the other hand, *Klebsiella* sp. 16S rDNA partial sequence has been deposited in Gen Bank with accession no. JN987862 by Fang (personal information), isolated in phenol-degrading activated sludge. In another study, *Klebsiella* sp. has been intentionally isolated as strains with high phenol degradation capability [29]. *Pseudomonas* sp. 16S rDNA partial sequence has been deposited in Gen Bank with accession no: HM192790, isolated from soil involving long-chain alkylphenols [30]. However, Shourian et al. [31] provided a few bacterial strains with a varied ability for utilizing phenol as the sole carbon source from pharmaceutical disposal wastewaters plant. Among the strains, *Pseudomonas* sp. as a potent phenol-degrading bacterium was identified and examined as having the greatest potential for degrading phenol.

4.2 Fluxes of organic matter, phenol and oxygen

The average fluxes of oxygen, phenol, and glucose in each period are provided in Tab. 2. The highest average O_2 flux was calculated to be 46.10 ± 11.4 g $O_2\,m^{-2}\,day^{-1}$ at period 5 while the total oxygen flux varied in the range of 26.10–59.80 g $O_2\,m^{-2}\,day^{-1}$; the oxygen fluxes for the oxidation of glucose and phenol varied between 15.95 and 47.90 g $O_2\,m^{-2}\,day^{-1}$ and between 1.31 and 11.90 g $O_2\,m^{-2}\,day^{-1}$, respectively. The highest fraction of oxygen was utilized for glucose degradation. Averaged over the entire time of reactor operation, the O_2 fluxes for glucose oxidation and phenol oxidation were 52–89% and 11–48% of the total O_2 flux, respectively. The O_2 flux for oxidation of phenol ($J_{O_2\text{-}2}$ in Tab. 2) was the highest (at around 40 g $O_2\,m^{-2}\,day^{-1}$) in the case of feeding with both phenol and glucose as carbon source, while the flux for phenol oxidation ($J_{O_2\text{-}2}$) responded most sensitively to O_2 pressure and fouling. The phenol flux directly depended on the O_2 pressure and initial phenol concentration in the case of feeding with only phenol as carbon source, as expected. In particular, the feeding was single carbon source based on phenol at periods 6–9. In these periods, the oxygen pressure was maintained at 0.54 atm. At period 6, the O_2 flux varied between 10.2 and 16.1 g $O_2\,m^{-2}\,day^{-1}$ while the averaged O_2 flux was 13.4 ± 2.2 g

CLEAN Soil Air Water

Figure 6. DGGE analysis of 16S rDNA amplified from MBfR consortium. A and B indicate periods 6 and 3, respectively.

$O_2\,m^{-2}\,day^{-1}$ at 10 mg/L of initial phenol concentration. In this period, the phenol loading per unit membrane surface area varied in the range of 4.26 to 6.77 g phenol $m^{-2}\,day^{-1}$ as the phenol flux was determined in the same values, which mean the complete removal of phenol. The phenol flux varied in the range of 5.8 to 21.2 g phenol $m^{-2}\,day^{-1}$ as the surface phenol loading was kept between 20.3 and 25.3 g phenol $m^{-2}\,day^{-1}$ at period 7. On the other hand, the total O_2 flux varied in a wide range of 13.9 and 50.5 g $O_2\,m^{-2}\,day^{-1}$. The average O_2 flux increased to about 25 ± 12.70 g $O_2\,m^{-2}\,day^{-1}$ with an increase of initial phenol concentration to 50 mg/L (period 7), while it decreased to about 21 ± 8.10 g $O_2\,m^{-2}\,day^{-1}$ with an increase of initial phenol concentration up to 100 mg/L (period 8). At period 9, even though the HRT was increased from 2.5 to 10 h, which means a decrease of phenol loading from 47.7 ± 1.5 g phenol $m^{-2}\,day^{-1}$ (period 8) to 12.5 ± 0.1 g phenol $m^{-2}\,day^{-1}$ (period 9), under same conditions at period 8, the total O_2 flux varied in the range of 1.5–11.0.

5 Conclusions

Phenol removal from solutions in the absence and presence of other organic carbon was studied using a lab scale MBfR with oxygen. Excellent removals of phenol and COD were obtained when initial phenol concentration was kept to 5 mg/L. However, an increase in the influent concentration of phenol from 10 to 100 mg/L caused a decrease in both phenol and COD removals. Additionally, it was observed that increasing the oxygen pressure did not contribute to an increase in the removal of phenol and COD. The flux for phenol oxidation responded most sensitively to O_2 pressure and membrane fouling. A low diversity containing *Dechloromonas* sp., *Klebsiella* sp., and *Pseudomonas* sp. as the main microbial species was established in the phenol-degrading MBfR.

6 Nomenclature

J	flux of the target compound, $g\,m^{-2}\,day^{-1}$
$J_{glucose}$	glucose flux, $g\,m^{-2}\,day^{-1}$
J_{phenol}	phenol flux, $g\,m^{-2}\,day^{-1}$
$J_{O_2\text{-}1}$	oxygen flux required to oxidize carbon, g $O_2\,m^{-2}\,day^{-1}$
$J_{O_2\text{-}2}$	oxygen flux required to oxidize phenol, g $O_2\,m^{-2}\,day^{-1}$
$J_{O_2\text{-}T}$	total flux of O_2, $g\,m^{-2}\,day^{-1}$
Q	influent flow rate, m^3/day
A_m	membrane (also biofilm) surface area, m^2
L_s	surface loading of contaminant, $g\,m^{-2}\,day^{-1}$
S_0	influent concentration of the compound, mg/L
S	effluent concentration of the compound, mg/L

The authors have declared no conflict of interest.

References

[1] A. Babuponnusami, K. Muthukumar, Degradation of Phenol in Aqueous Solution by Fenton, Sono-Fenton and Sono-photo-Fenton Methods, *Clean – Soil Air Water* **2011**, *39*, 142–147.

[2] M. L. Leong, K. M. Lee, S. O. Lai, B. S. Ooi, Sludge Characteristics and Performances of the Sequencing Batch Reactor at Different Influent Phenol Concentrations, *Desalination* **2011**, *270*, 181–187.

[3] I. A. Vasiliadou, G. Tziotzios, D. V. Vayenas, A Kinetic Study of Combined Aerobic Biological Phenol and Nitrate Removal in Batch Suspended Growth Cultures, *Int. Biodeterior. Biodegrad.* **2008**, *61*, 261–271.

[4] Council Directive 98/83/EC, *Off. J. Eur. Commun.* **1998**, *L330*, 32–54.

[5] O. Abdelwahab, N. K. Amin, E. S. Z. El-Ashtoukhy, Electrochemical Removal of Phenol from Oil Refinery Wastewater, *J. Hazard. Mater.* **2009**, *163*, 711–716.

Table 2. The average values of fluxes and loadings of phenol and glucose at each periods

Period no.	$L_{s\text{-}glucose}$ $g\,m^{-2}\,day^{-1}$	$L_{s\text{-}phenol}$ $g\,m^{-2}\,day^{-1}$	$J_{glucose}$ $g\,m^{-2}\,day^{-1}$	J_{phenol} $g\,m^{-2}\,day^{-1}$	$J_{O_2\text{-}1}$ g $O_2\,m^{-2}\,day^{-1}$	$J_{O_2\text{-}2}$ g $O_2\,m^{-2}\,day^{-1}$	$J_{O_2\text{-}2}/J_{O_2\text{-}T}$
1	12.2 ± 2.5	0.64 ± 0.18	5.04 ± 2.40	0.43 ± 0.20	5.37 ± 5.00	0.87 ± 0.68	11.6 ± 5.46
2	13.0 ± 1.5	0.60 ± 0.10	11.8 ± 2.70	0.6 ± 0.10	12.5 ± 3.40	1.4 ± 0.2	10.8 ± 3.80
3	18.4 ± 3.4	2.5 ± 0.12	12.6 ± 5.6	2.0 ± 0.35	13.4 ± 3.2	4.8 ± 0.89	29 ± 8.60
4	49.8 ± 9.2	4.6 ± 0.77	23.6 ± 5.5	2.7 ± 1.50	25.0 ± 16.3	6.8 ± 4.1	51.4 ± 39.3
5	55.2 ± 5	4.7 ± 1.3	38.1 ± 10.60	2.4 ± 1.10	40.4 ± 13.00	5.6 ± 4.5	12.2 ± 7.50
6	–	5.6 ± 0.9	–	5.6 ± 0.90	–	13.4 ± 2.2	100
7	–	23.1 ± 2.5	–	10.5 ± 5.50	–	24.9 ± 12.70	100
8	–	47.7 ± 1.5	–	8.7 ± 4.50	–	20.8 ± 8.10	100
9	–	12.5 ± 0.1	–	2.3 ± 2.20	–	5.6 ± 4.60	100

[6] S. Nosrati, N. S. Jayakumar, M. A. Hashim, Extraction Performance of Chromium(VI) with Emulsion Liquid Membrane by Cyanex 923 as Carrier Using Response Surface Methodology, *Desalination* **2011**, *266*, 286–290.

[7] K. Turhan, S. Uzman, Removal of Phenol from Water Using Ozone, *Desalination* **2008**, *229*, 257–263.

[8] G. Zelmanov, R. Semiat, Phenol Oxidation Kinetics in Water Solution Using Iron(3)-Oxide-Based Nano-Catalysts, *Water Res.* **2008**, *42*, 3848–3856.

[9] A. Uygur, F. Kargı, Phenol Inhibition of Biological Nutrient Removal in a Four-Step Sequencing Batch Reactor, *Process Biochem.* **2004**, *39*, 2123–2128.

[10] G. Moussavi, B. Barikbin, M. Mahmoudi, The Removal of High Concentrations of Phenol from Saline Wastewater Using Aerobic Granular SBR, *Chem. Eng. J.* **2010**, *158*, 498–504.

[11] R. J. A. L'Amour, E. B. Azevedo, S. G. F. Leite, M. Dezotti, Removal of Phenol in High Salinity Media by a Hybrid Process (Activated Sludge + Photocatalysis), *Sep. Purif. Technol.* **2008**, *60*, 142–146.

[12] A. Dixit, A. J. Tirpude, A. K. Mungray, M. Chakraborty, Degradation of 2,4 DCP by Sequential Biological-Advanced Oxidation Process Using UASB and UV/TiO_2/H_2O_2, *Desalination* **2011**, *272*, 265–269.

[13] C. Trigo, J. L. Campos, J. M. Garrido, R. Méndez, Start-Up of the Anammox Process in a Membrane Bioreactor, *J. Biotechnol.* **2006**, *126*, 475–487.

[14] J. Dosta, J. M. Nietoi, J. Vila, M. Grifoll, J. Mata-Alvarez, Phenol Removal from Hypersaline Wastewaters in a Membrane Biological Reactor (MBR): Operation and Microbiological Chracterization, *Bioresour. Technol.* **2011**, *102*, 4013–4020.

[15] I. N. Sgountzos, S. Pavlou, C. A. Paraskeva, A. C. Payatake, Growth Kinetics of *Pseudomonas fluorescens* in Sand Beds during Biodegradation of Phenol, *Biochem. Eng. J.* **2006**, *30*, 164–173.

[16] E. Syron, E. Casey, Membrane-Aerated Biofilms for High Rate Biotreatment: Performance Apprasial, Engineering Principles, Scale-Up, and Development Requirements, *Environ. Sci. Technol.* **2008**, *42*, 1833–1844.

[17] H. Hasar, Simultaneous Removal of Organic Matter and Nitrogen Compounds by Combining a Membrane Bioreactor and a Membrane Biofilm Reactor, *Bioresour. Technol.* **2009**, *100*, 2699–2705.

[18] H. Hasar, S. Xia, H. A. Chang, B. E. Rittmann, Simultaneous Removal of Organic Matter and Nitrogen Compounds by an Aerobic/Anoxic Membrane Biofilm Reactor, *Water Res.* **2008**, *42*, 4109–4116.

[19] J. H. Hwang, N. Çiçek, J. A. Oleszkiewicz, Achieving Biofilm Control in a Membrane Biofilm Reactor Removing Total Nitrogen, *Water Res.* **2010**, *44*, 2283–2291.

[20] E. Syron, H. Kelly, E. Casey, Studies on the Effect of Concentration of a Self-Inhibitory Substrate on Biofilm Reaction Rate under Co-Diffusion and Counter Diffusion Configurations, *J. Membr. Sci.* **2009**, *335*, 76–82.

[21] H. Hasar, U. Ipek, Gas Permeable-Membrane for Hydrogenotrophic Denitrification, *Clean – Soil Air Water* **2010**, *38*, 23–26.

[22] APHA, *Standard Methods for the Examination of Water and Wastewater*, American Public Health Association, Washington DC **1995**.

[23] R. K. Gupta, F. Yakuphanoglu, H. Hasar, A. A. Al-Khedhairy, p-Si/DNA Photoconductive Diode for Optical Sensor Applications, *Synth. Metals* **2011**, *161*, 2011–2016.

[24] A. Barrios-Martinez, E. Barbot, B. Marrot, P. Moulin, N. Roche, Degradation of Phenol-Containing Wastewaters by MBR, *J. Membr. Sci.* **2006**, *281*, 288–296.

[25] E. Casey, B. Glennon, G. Hamer, Oxygen Mass Transfer Characteristics in a Membrane-Aerated Biofilm Reactor, *Biotechnol. Bioeng.* **1999**, *62*, 183–192.

[26] H. Satoh, H. Ono, B. Rulin, J. Kamo, S. Okabe, K.-I. Fukushi, Macroscale and Microscale Analyses of Nitrification and Denitrification in Biofilms Attached on Membrane Aerated Biofilm Reactors, *Water Res.* **2004**, *38*, 1633–1641.

[27] L. S. Downing, R. Nerenberg, Effect of Oxygen Gradients on the Activity and Microbial Community Structure of a Nitrifying. Membrane-Aerated Biofilm, *Biotechnol. Bioeng.* **2008**, *101*, 1193–1204.

[28] R. Nerenberg, Y. Kawagoshi, B. E. Rittmann, Kinetics of a Hydrogen-Oxidizing, Perchlorate-Reducing Bacterium, *Water Res.* **2006**, *40*, 3290–3296.

[29] B.-Y. Chen, W.-M. Chen, Y.-P. Wu, C.-C. Hsueh, K.-L. Lin, C.-T. Chang, Revealing Phenol Tolerance of Indigenous Phenol Degraders Isolated from Northeast Taiwan, *J. Taiwan Inst. Chem. Eng.* **2010**, *41*, 636–643.

[30] N. N. Tuan, H. C. Hsieh, Y. W. Lin, S. L. Huang, Analysis of Bacterial Degradation Pathways for Long-Chain Alkylphenols Involving Phenol Hydroxylase, Alkylphenol Monooxygenase and Catechol Dioxygenase Genes, *Bioresour. Technol.* **2011**, *102*, 4232–4240.

[31] M. Shourian, K. A. Noghabi, H. S. Zahiri, T. Bagheri, G. Karballaei, M. Mollaei, I. Rad, et al., Efficient Phenol Degradation by a Newly Characterized *Pseudomonas* sp. SA01 Isolated from Pharmaceutical Wastewaters, *Desalination* **2009**, *246*, 577–594.